

# Synthesis and single-crystal X-ray diffraction studies of new framework substituted type II clathrates, $\text{Cs}_8\text{Na}_{16}\text{Ag}_x\text{Ge}_{136-x}$ ( $x < 7$ )

M. Beekman<sup>a</sup>, W. Wong-Ng<sup>b</sup>, J.A. Kaduk<sup>c</sup>, A. Shapiro<sup>b</sup>, G.S. Nolas<sup>a,\*</sup>

<sup>a</sup>Department of Physics, University of South Florida, 4202 East Fowler Ave., PHY 114, Tampa, FL 33620, USA

<sup>b</sup>Materials Science and Engineering Laboratory, National Institute of Standards and Technology, Gaithersburg, MD 20899, USA

<sup>c</sup>INEOS Technologies, Naperville, IL 60566, USA

Received 31 October 2006; received in revised form 2 January 2007; accepted 4 January 2007

Available online 14 January 2007

## Abstract

New inorganic type II clathrates with Ag atoms substituting for framework Ge atoms,  $\text{Cs}_8\text{Na}_{16}\text{Ag}_x\text{Ge}_{136-x}$  ( $x = 0, 5.9, \text{ and } 6.7$ ), have been synthesized by reaction of the pure elements at high temperature. Structural refinements have been performed using single crystal X-ray diffraction. The materials crystallize with the cubic type II clathrate crystal structure (space group  $Fd\bar{3}m$ ) with  $a = 15.49262(9)$  Å,  $15.51605(6)$  Å, and  $15.51618(9)$  for  $x = 0, 5.9, \text{ and } 6.7$ , respectively, and  $Z = 1$ . The structure is formed by a covalently bonded Ag–Ge framework, in which the Cs and Na atoms are found inside two types of polyhedral cages. Ag substitutes for Ge in the tetrahedrally bonded framework positions, and was found to preferentially occupy the most asymmetric  $96g$  site. The proven ability to substitute atoms for the germanium framework should offer a route to the synthesis of new compositions of type II clathrates, materials that are of interest for potential thermoelectrics applications.

© 2007 Elsevier Inc. All rights reserved.

**Keywords:** Clathrate; Framework compound; Single crystal X-ray diffraction; Ag; Ge

## 1. Introduction

Inorganic clathrate compounds, first discovered over 40 years ago [1], comprise a class of materials which display a rich variety of chemical and physical properties. The primary characteristic of all clathrates is an open-structured “host” framework, typically of Si, Ge, or Sn, that has the ability to encage another species of “guest” atom or molecule. The unique structural features as well as guest–host relationship in many of these materials results in unique and diverse properties, including semiconducting and metallic behavior [2], enhanced thermoelectric properties [3–5], very low thermal conductivities [6], superconductivity [7], magnetism [8,9], and theoretically ultra-hard materials [10]. Clathrates crystallize in several structure types, and also with some superstructure variants [11,12]. Overwhelmingly, clathrates with the type I structure have been the most extensively investigated, in

large part due to the superconducting [7] and enhanced thermoelectric properties [3–5] that some type I clathrates exhibit.

Another structure type of clathrates that is receiving increased attention, particularly as potential thermoelectric materials [4], are those possessing the type II structure (see Fig. 1). Although some structural similarities exist between type I and II clathrates, several important differences are apparent, notably the ability to vary the guest content in the latter [2], whereas in the former the structure is empirically fixed at full occupation. The type II clathrate structure (Fig. 1) is composed of two distinct framework-forming polyhedra (see Fig. 2), eight larger hexakaidecahedra ( $E_{28}$ ) and 16 smaller pentagonal dodecahedra ( $E_{20}$ ) per conventional unit cell, and the general chemical formula may be written as  $A_8B_{16}E_{136}$  ( $A, B =$  guest atoms;  $E =$  Si, Ge, or Sn). These polyhedra act as structural building blocks, sharing faces to form the type II clathrate crystal structure. There are three distinct crystallographic sites in the type II clathrate framework, the  $96g$  (also denoted as  $E1$  herein),  $32e$  ( $E2$ ), and  $8a$  ( $E3$ ) using the

\*Corresponding author. Fax: +1 813 974 5813.

E-mail address: [gnolas@cas.usf.edu](mailto:gnolas@cas.usf.edu) (G.S. Nolas).

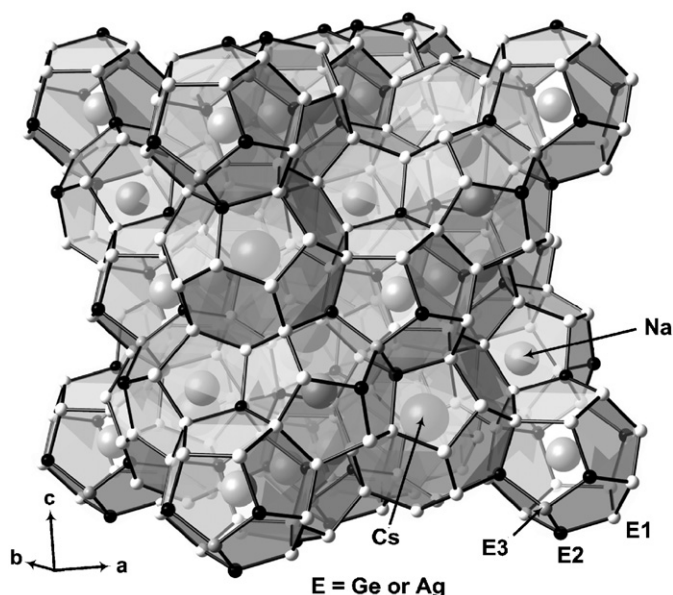


Fig. 1. The cubic type II clathrate crystal structure, emphasizing the framework-building polyhedra. The Na, Cs, and framework sites are labeled.

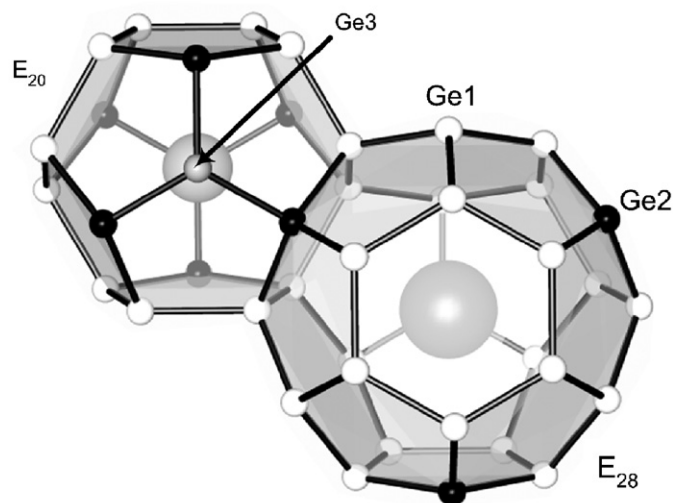


Fig. 2. The  $E_{20}$  and  $E_{28}$  polyhedra that form the  $\text{Cs}_8\text{Na}_{16}\text{Ag}_x\text{Ge}_{136-x}$  type II clathrate framework. The  $8a$  (grey),  $32e$  (black), and  $96g$  (white) sites are labeled as in the text.

Wyckoff notation. There are two distinct guest atom sites, the  $8b$  site inside the larger  $E_{28}$  cage, and the  $16c$  site inside the smaller  $E_{20}$  cage.

To date, only a small set of compositions have been reported for inorganic type II clathrates. These include (with references given only for the first published reports of each composition)  $\text{Na}_x\text{E}_{136}$  ( $E = \text{Si}, \text{Ge}$ ;  $0 < x < 24$ ) [1,2],  $\text{Cs}_7\text{Si}_{136}$  [2],  $\text{A}_8\text{Na}_{16}\text{E}_{136}$  ( $A = \text{Cs}, \text{Rb}$ ;  $E = \text{Si}, \text{Ge}$ ) [13],  $\text{Ba}_8\text{Na}_{16}\text{Si}_{136}$  [14],  $\text{Ba}_{16}\text{Ga}_{32}\text{Sn}_{104}$  [15],  $\text{Cs}_8\text{Ge}_{136}$  [16], and the completely guest-free clathrates  $\text{Si}_{136}$  [17] and  $\text{Ge}_{136}$  [18]. Indeed, with the exception of  $\text{Ba}_{16}\text{Ga}_{32}\text{Sn}_{104}$  [15], no investigation has been made into the stability of type II clathrates under substitution of the framework atoms by

other species. Herein we report the synthesis and X-ray single crystal structural studies of new framework substituted type II germanium clathrates,  $\text{Cs}_8\text{Na}_{16}\text{Ag}_x\text{Ge}_{136-x}$  ( $x = 0, 5.9, \text{ and } 6.7$ ).

## 2. Experimental<sup>1</sup>

### 2.1. Synthesis

The three samples studied in this work were synthesized as follows. High-purity Cs metal (99.98%, Alfa Aesar), Na metal (99.95%, Alfa Aesar), Ag powder (99.9%, Alfa Aesar), and Ge powder (ground to 325 mesh from intrinsic crystalline Ge), were combined in tungsten crucibles, after thoroughly premixing the Ag and Ge powders. The crucibles were then sealed under nitrogen inside steel canisters, which were in turn sealed in quartz ampoules. The mixtures were held at  $800^\circ\text{C}$  for 2 days, and then annealed at  $650^\circ\text{C}$  for 7 days. The products consisted of small ( $\approx 0.5$  mm in size) crystals possessing a metallic luster that are stable toward both air and water. Target  $\text{Cs}_8\text{Na}_{16}\text{Ag}_x\text{Ge}_{136-x}$  stoichiometries of  $x = 0$  (Sample I), 5 (Sample II), and 8 (Sample III) were attempted, however as discussed below Ag contents greater than  $x = 7$  were currently not achieved. Small ( $\approx 0.1$  mm in size) single crystals were cut from the larger aggregates for single crystal diffraction measurements. The compositions of the crystals used were also analyzed using energy dispersive spectroscopy (EDS).

### 2.2. Structure determination

The structures of the  $\text{Cs}_8\text{Na}_{16}\text{Ag}_x\text{Ge}_{136-x}$  crystals were determined using single crystals mounted on Lindemann-type glass fibers in random orientations. Data were collected at 298 K with  $\text{MoK}_\alpha$  radiation on a computer-controlled  $\kappa$ -axis diffractometer equipped with a graphite crystal incident beam monochromator.  $\text{MoK}_\alpha$  radiation ( $0.71073 \text{ \AA}$ ) and a Zr filter were used. Preliminary cell constants and orientation matrices for data collection were obtained from least-squares refinements using setting angles of 25 reflections ( $18^\circ < \theta < 25^\circ$ ). The final lattice parameters of the three  $\text{Cs}_8\text{Na}_{16}\text{Ag}_x\text{Ge}_{136-x}$  samples were obtained from X-ray powder diffraction using the Rietveld refinement method (GSAS Suite) [19–21]. The reported structure of  $\text{Cs}_8\text{Na}_{16}\text{Ge}_{136}$  [13,22] was employed as a starting model.

Table 1 gives the details of the experimental and structural solution for the three crystals. The  $\omega/2\theta$  scan method was used for data collection. During the data

<sup>1</sup>Certain commercial equipment, instruments, or materials are identified in this paper in order to specify the experimental procedure adequately. Such identification is not intended to imply recommendation or endorsement by the Air Force Research Laboratory or the National Institute of Standards and Technology, nor is it intended to imply that the materials or equipment identified are necessarily the best available for the purpose.

Table 1  
Summary of data collection for the three compositions of  $\text{Cs}_8\text{Na}_{16}\text{Ag}_x\text{Ge}_{136-x}$

	Sample I ( $x = 0$ )	Sample II ( $x = 5.9$ )	Sample III ( $x = 6.7$ )
Color	Gray (metallic)	Gray (metallic)	Gray (metallic)
Radiation, graphite Monochromator	Mo, 0.7107 Å	Mo, 0.7107 Å	Mo, 0.7107 Å
Crystal size	0.10 × 0.11 × 0.14 mm	0.09 × 0.13 × 0.15 mm	0.08 × 0.11 × 0.17 mm
Data collection			
Standard reflections			
Intensity monitor	888	–3–13–3	–3–13–3
	10 100	88–8	888
	10 60	10 100	–100–10
Orientation monitor	888	10 100	40 16
	1640	40 16	11 11 5
	1060	5 15 5	5 15 5
# Reflections measured			
Total	1627	2252	2409
Independent	352	474	505
Refinement	311 ( $>4\sigma$ )	403 ( $>4\sigma$ )	397 ( $>4\sigma$ )
$2\theta$ range (°)	2–64	2–72	2–72
Range of $h, k, \ell$	$0 < h, k, \ell < 23$	$0 < h, k, \ell < 25$	$0 < h, k, \ell < 26$
Range of transmission factors	0.15–0.23	0.11–0.25	0.14–0.30

collection process, three reflections were employed to monitor the stability of the crystal, and another three to monitor the orientation. All three crystals were found to be stable chemically and mechanically with respect to X-ray. Lorentz and polarization corrections (CAD4 manual [23]) were applied. At the end of data collection, three reflections with  $\chi$  angles near  $90^\circ$  were measured as a function of the  $\phi$  angle in order to obtain the empirical adsorption correction curve.

The data were reduced and the structures were refined using the PC version of SHELXTL [24]. The initial model used for least-squares refinements was that of  $\text{Cs}_8\text{Na}_{16}\text{Ge}_{136}$  [13,22]. The cell parameters were obtained from the powder diffraction data and have been used for the structure refinements. Full matrix least-squares refinements on structure factors ( $F^2$ ) (function minimized:  $1/[\sigma^2(F_o^2) + (AP)^2 + BP]$ , where  $P = (\max F_o^2 + 2F_c^2)/3$ ) was carried out. Atomic scattering factors were taken from the International Tables for Crystallography [25]. A summary of the data collection is given in Table 1.

### 3. Results and discussion

#### 3.1. Structure and bonding in $\text{Cs}_8\text{Na}_{16}\text{Ag}_x\text{Ge}_{136-x}$

Powder X-ray diffraction patterns for the three  $\text{Cs}_8\text{Na}_{16}\text{Ag}_x\text{Ge}_{136-x}$  samples are presented in Fig. 3. All patterns are characteristic of the type II clathrate crystal structure, and indicate the phase purity of the samples. As shown in the inset of Fig. 3, a very small amount of elemental Ag was found to be present in Sample III. This is consistent with single-crystal X-ray diffraction and EDS measurements discussed below, which found the value of  $x$  for Sample III to be less than the target value of 8.

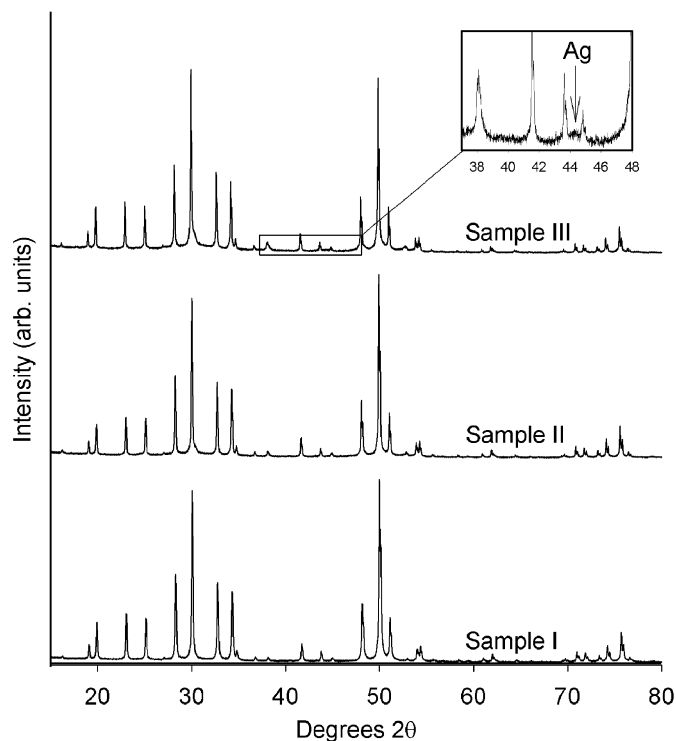


Fig. 3. Powder X-ray diffraction patterns for the  $\text{Cs}_8\text{Na}_{16}\text{Ag}_x\text{Ge}_{136-x}$  samples: Sample I ( $x = 0$ ), Sample II ( $x = 5.9(1.0)$ ), and Sample III ( $x = 6.7(1.1)$ ). The inset is a magnification showing the trace amount of elemental Ag present in Sample III.

As confirmed by single crystal and powder X-ray diffraction measurements, all three samples crystallized with the cubic type II clathrate structure (space group  $Fd\bar{3}m$ ). Summaries of the single crystal X-ray data collection and refinement results are given in Tables 1

and 2. The refined atomic positions, occupancies, and thermal parameters are given in Table 3. The Na atoms were found to exclusively occupy the smaller Ge<sub>20</sub> dodecahedra, while the Cs atoms occupy the larger Ge<sub>28</sub> hexacaidecahedra. No mixing of the cation guests was observed at these sites, both of which were also found to be fully occupied from the single crystal structural refinement. As was originally observed by Bobev and Sevov [13], stabilization of the clathrate structure is facilitated by “matching” cation and cage sizes, thus the smaller Na and larger Cs reside in the smaller Ge<sub>20</sub> and larger Ge<sub>28</sub> polyhedra, respectively.

The lattice parameters of the Cs<sub>8</sub>Na<sub>16</sub>Ag<sub>x</sub>Ge<sub>136–x</sub> clathrates increase with increasing Ag content, indicating a slight expansion of the framework upon substituting Ag

for Ge. The lattice parameters for Samples II and III are only marginally different, consistent with the small difference in Ag content. We note that the lattice parameter of the Cs<sub>8</sub>Na<sub>16</sub>Ge<sub>136</sub> sample in the present work ( $x = 0$ ,  $a = 15.49262(9)$  Å) is slightly higher than that reported in Ref. [13] ( $a = 15.4805(6)$  Å). We also note that the synthesis method of the current work differs somewhat from that of Ref. [13].

Empirically, transition metals have only been observed to occupy positions on the framework of type I clathrates [26]. For completeness, the possibility of Ag substitution at the guest positions of the type II clathrates in the present study was systematically ruled out during preliminary structural refinements, and the single crystal X-ray diffraction data indicate Ag substitutes exclusively for Ge on the Ge framework. All Ge/Ag sites in the present study of the Cs<sub>8</sub>Na<sub>16</sub>Ag<sub>x</sub>Ge<sub>136–x</sub> clathrates were refined with a total occupancy constrained to unity. As noted from the site occupancies in Table 3, Ag shows a preference for substitution on the 96*g* site. For Sample II ( $x = 5.9(1.0)$ ), substitution is found exclusively on the E1 (96*g*) site. For Sample III ( $x = 6.7(1.1)$ ), the majority of the Ag again substitutes on this site ( $\approx 70\%$  of the total Ag content), though 4.8% and 6.5% of the 96*g* and 32*e* sites, respectively, are occupied by Ag.

Preferential occupation of substituting species has also been observed in type I clathrates, and several structural studies have revealed a preference for the 6*c* site in these compounds [26–28]. In particular, transition metals substituting for silicon and germanium were found to preferentially occupy the 6*c* site [26], which is the most symmetric of the type I clathrate framework sites. The 6*c* sites in the type I clathrates are located on hexagonal

Table 2  
Crystal data and structure refinement for Cs<sub>8</sub>Na<sub>16</sub>Ag<sub>x</sub>Ge<sub>136–x</sub> (at 25 °C)

	Sample I ( $x = 0$ )	Sample II ( $x = 5.9$ )	Sample III ( $x = 6.7$ )
<i>Crystal data</i>			
Space group	$Fd\bar{3}m$ (No.227)	$Fd\bar{3}m$ (No.227)	$Fd\bar{3}m$ (No.227)
Cell constant			
$a$ (powder)	15.49262(9) Å	15.51605(6) Å	15.51618(9) Å
$V$	3718.56(4) Å <sup>3</sup>	3735.46(2) Å <sup>3</sup>	3735.55(3) Å <sup>3</sup>
Formula unit/ unit cell ( $Z$ )	1	1	1
<i>Least-squares refinements</i>			
$WR(F^2)$	0.0571	0.070	0.064
$R_1$	0.024 (311 refl.)	0.027 (403 refl.)	0.029 (397 refl.)
$R_2$	0.031 (352 refl.)	0.036 (474 refl.)	0.044 (505 refl.)
Goodness of fit	1.159	1.060	1.130

Table 3  
Atomic coordinates and isotropic atomic displacement parameters for the three Cs<sub>8</sub>Na<sub>16</sub>Ag<sub>x</sub>Ge<sub>136–x</sub> compositions ( $Fd\bar{3}m$ , No. 227; origin chosen at center ( $\bar{3}m$ ))

Atom	Multiplicity	Wyckoff letter	Site symm	Occ.	$x$	$y$	$z$	$U_{iso}$ (Å <sup>2</sup> )
<i>Sample I, <math>x = 0</math></i>								
Cs	8	$b$	$\bar{4}3m$	1.0	3/8	3/8	3/8	0.0352(3)
Na	16	$c$	$\bar{3}m$	1.0	0	0	0	0.0364(11)
Ge1	96	$g$	$m$	1.0	0.06783(2)	0.06783(2)	0.37033(2)	0.0116(2)
Ge2	32	$e$	$3m$	1.0	0.21761(2)	0.21761(2)	0.21761(2)	0.0110(1)
Ge3	8	$a$	$\bar{4}3m$	1.0	1/8	1/8	1/8	0.0103(3)
<i>Sample II, <math>x = 5.9(1.0)</math></i>								
Cs	8	$b$	$\bar{4}3m$	1.0	3/8	3/8	3/8	0.0402 (4)
Na	16	$c$	$\bar{3}m$	1.0	0	0	0	0.0413(13)
Ge1/Ag	96	$G$	$m$	.938(10)/.062(10)	0.06771(2)	0.06771(2)	0.37045(2)	0.00951(14)
Ge2	32	$e$	$3m$	1.0	0.21755(2)	0.21755(2)	0.21755(2)	0.0092(2)
Ge3	8	$a$	$\bar{4}3m$	1.0	1/8	1/8	1/8	0.0092(3)
<i>Sample III, <math>x = 6.7(1.1)</math></i>								
Cs	8	$b$	$\bar{4}3m$	1.0	3/8	3/8	3/8	0.0335(4)
Na	16	$c$	$\bar{3}m$	1.0	0	0	0	0.0348(15)
Ge1/Ag1	96	$g$	$m$	.952(8)/.048(8)	0.06767(2)	0.06767(2)	0.37043(2)	0.0029(2)
Ge2/Ag2	32	$e$	$3m$	.935(12)/.065(12)	0.21751(3)	0.21751(3)	0.21751(3)	0.0037(2)
Ge3	8	$a$	$\bar{4}3m$	1.0	1/8	1/8	1/8	0.0021(3)

Table 4  
Bond distances (Å) in  $\text{Cs}_8\text{Na}_{16}\text{Ag}_x\text{Ge}_{136-x}$

<i>x</i>	Atoms	Distance	Atoms	Distance
<i>Sample I</i>				
0.0	Cs–Ge1	$4.1395(4) \times 12$	Ge1–Ge1	$2.5006(4) \times 2$
	Cs–Ge1	$4.2255(11) \times 12$	Ge1–Ge1	2.5051(9)
	Cs–Ge2	$4.2235(11) \times 4$	Ge1–Ge2	2.4902(4)
	Na–Ge1	$3.5419(2) \times 12$	Ge2–Ge1	$2.4903(4) \times 3$
	Na–Ge2	$3.4452(3) \times 6$	Ge2–Ge3	2.4850(6)
	Na–Ge3	$3.3543(0) \times 2$	Ge3–Ge2	$2.4850(5) \times 4$
<i>Sample II</i>				
5.9(1.0)	Cs–Ge1/Ag1	$4.1448(3) \times 12$	Ge1/Ag1–Ge1/Ag1	$2.5013(4) \times 2$
	Ge1/Ag1–Cs	$4.2293(4) \times 12$	Ge1/Ag1–Ge1/Ag1	2.5142(8)
	Ge2–Cs	$4.2315(6) \times 4$	Ge1/Ag1–Ge2	2.4955(4)
	Na–Ge1/Ag1	$3.5492(2) \times 12$	Ge2–Ge1/Ag1	$2.4955(4) \times 3$
	Na–Ge2	$3.4497(2) \times 6$	Ge2–Ge3	2.4871(6)
	Na–Ge3	$3.3593(0) \times 2$	Ge3–Ge2	$2.4871(6) \times 4$
<i>Sample III</i>				
6.7(1.1)	Cs–Ge1/Ag1	$4.1454(4) \times 12$	Ge1/Ag1–Ge1/Ag1	$2.5010(4) \times 2$
	Ge1/Ag1–Cs	$4.2285(5) \times 12$	Ge1/Ag1–Ge1/Ag1	2.5159(10)
	Ge2/Ag2–Cs	$4.2326(7) \times 4$	Ge1/Ag1–Ge2/Ag2	2.4952(5)
	Ge1/Ag1–Na	$3.5493(3) \times 12$	Ge2/Ag2–Ge1/Ag1	$2.4952(5) \times 3$
	Na–Ge2/Ag2	$3.4494(3) \times 6$	Ge2/Ag2–Ge3	2.4861(7)
	Na–Ge3	$3.3594(0) \times 2$	Ge3–Ge2/Ag2	$2.4861(7) \times 4$

six-member rings of framework atoms. The E1 (96*g*) sites in the type II clathrate structure, which the Ag atoms are found to preferentially occupy, in fact constitute all of the hexagonal six-member sites (see Figs. 1 and 2), whereas the 6*c* sites in type I clathrates comprise only one third of the hexagonal ring sites. In contrast to the 6*c* sites of the type I clathrates, the 96*g* sites are the least symmetric site of the framework in the type II structure (discussed further below).

We next offer a qualitative discussion of the cage environments of the alkali guests in the  $\text{Cs}_8\text{Na}_{16}\text{Ag}_x\text{Ge}_{136-x}$  samples. The relevant bond distances in  $\text{Cs}_8\text{Na}_{16}\text{Ag}_x\text{Ge}_{136-x}$  are given in Table 4. In  $\text{Cs}_8\text{Na}_{16}\text{Ag}_x\text{Ge}_{136-x}$ , Na resides in the smaller 20-membered cage with Na–Ge/Ag distances ranging from 3.3543(0) to 3.5419(2) Å for Sample I; from 3.3593(0) to 3.5492(2) Å for Sample II; and from 3.3594(0) to 3.5493(3) Å for Sample III. The larger Cs were found to reside inside the larger 28-membered cage, with Cs–Ge/Ag distances ranging from 4.1395(4) to 4.2255(11) Å for Sample I; 4.1448(3) to 4.2315(6) Å for Sample II; and 4.1454(4) to 4.2326(7) Å for Sample III. The shortest Cs–Ge and Na–Ge distances in the three compounds are 4.1395(4) and 3.3543(0) Å, respectively, and both were found in the non-substituted  $\text{Cs}_8\text{Na}_{16}\text{Ge}_{136}$  sample. Subtracting from these distances the single-bond radius of Ge (1.225 Å) [29], the values become 2.915 and 2.129 Å for Cs–Ge and Na–Ge, respectively. This provides a rough measure of the amount of “space” inside the respective cages. If we instead subtract the single-bond radius for Ag (1.412 Å) [29] from these guest–framework distances, we obtain 2.728 and 1.942 Å for Cs–Ag and Na–Ag, respectively. Assuming the alkali guests to be singly ionized [13] (i.e.  $\text{Na}^+$  and  $\text{Cs}^+$ ), we may take the approximate ionic radii for Cs and Na to be 1.70 and 1.02 Å, respectively [30]. Using this

simple estimate of the available space inside the framework polyhedra, these alkali metals can “fit” into the type II cavities quite easily, with some excess space. As shown in Table 3, the refined atomic displacement parameters ( $U_{\text{iso}}$ ) for the Cs and Na guests in the  $\text{Cs}_8\text{Na}_{16}\text{Ag}_x\text{Ge}_{136}$  samples are both significantly larger than those for the framework Ge/Ag atoms,<sup>2</sup> in agreement with those previously reported for  $\text{Cs}_8\text{Na}_{16}\text{Ge}_{136}$  [13,31]. The larger  $U_{\text{iso}}$  for Cs and Na can be attributed to the weaker bonding between guest and framework, allowing for relatively large thermal motion of the guest atoms inside their framework cages [31]. Indeed, the thermal motion of Cs in the larger cage of these clathrates corresponds to an optic vibrational mode [32]. The presence of such loosely bound guest atoms in type I clathrate materials results in the very low lattice thermal conductivities some clathrates possess [6], which can be attributed to the scattering of the heat carrying acoustic phonons by the localized, incoherent guest vibration modes. Recent experimental [33] and theoretical [34] results suggest a similar effect may occur in type II clathrates, and from the large  $U_{\text{iso}}$  values for the alkali guests we expect the lattice thermal conductivities of  $\text{Cs}_8\text{Na}_{16}\text{Ag}_x\text{Ge}_{136-x}$  clathrates should be quite low.

The Ge–Ge distances in the three  $\text{Cs}_8\text{Na}_{16}\text{Ag}_x\text{Ge}_{136-x}$  compounds (in the range of 2.4850(4)–2.5159(10) Å) are somewhat longer than that in elemental Ge (2.445 Å), where strong tetrahedral bonds are expected. As one compares the corresponding bond lengths in the three  $\text{Cs}_8\text{Na}_{16}\text{Ag}_x\text{Ge}_{136-x}$  compositions (Table 4), one observes

<sup>2</sup>The fact that the  $U_{\text{iso}}$  of the framework sites (E1, E2, and E3) for Sample III are notably smaller than for Samples I and II is likely due to the quality of the crystals (e.g. surface roughness) as well as possible effects from the approximate absorption correction used.

that in general the compositions with Ag substitution give rise to longer bond lengths as compared to those of  $\text{Cs}_8\text{Na}_{16}\text{Ge}_{136}$ . However, the corresponding bond distances in compositions II and III are not significantly different (consistent with their somewhat similar lattice parameters).

Table 5 gives the selected bond angles surrounding the Ge/Ag sites. In  $\text{Cs}_8\text{Na}_{16}\text{Ge}_{136}$ , each Ge is bonded to four other Ge atoms; schematics showing the local bonding environments of the Ge1 (96g), Ge2 (32e), and Ge3 (8a) sites are given in Fig. 4. The Ge3 (8a) site has four equal bonds and six equal bond angles and therefore it is the most symmetric site (and also has the strongest Ge–Ge bond among the three Ge sites). The Ge2 (32e) site has two different sets of angles, and by comparison with the Ge3 (8a) site it is relatively more distorted (or more strained). Around Ge1 (96g), while five of the angles are close to tetrahedral, the sixth is close to  $120^\circ$ , and forms the internal angle of the hexagonal face of the  $\text{E}_{28}$  cage. (Recall six Ge1 link together to form the hexagonal face of the polyhedra in the  $\text{Cs}_8\text{Na}_{16}\text{Ge}_{136}$  structure.) Therefore the local bonding environment around the Ge1 (96g) site is the most “distorted” of the three framework sites, and is expected to be the most susceptible for substitution. Our single crystal X-ray refinement results support this conclusion, as preference is found for substitution at the Ge1 (96g) site. Also, from Table 4, we note that the bond distances surrounding the Ge1 site are slightly larger than the others

in the structure, indicating slightly weaker bonding around this site. Although the presence of the *d*-orbitals of Ag may also affect the bonding geometry, our results indicate that the substitution of Ag does not have a significant effect on the geometry around the Ge/Ag sites (Table 5).

### 3.2. Composition

Results of SEM analysis confirmed the presence of Ag within the clathrate crystals. Severe overlap of the Na K (1.041 keV) and Ge L (1.096 keV) makes accurate measurements of the Na composition extremely difficult, thus it has been assumed that the Na contribution to the compositions is  $\approx 10\text{at}\%$  in all compounds, an assumption that is supported by the structure determination results that there are no vacancy sites in the structure.

The composition of Sample II as determined from EDS was  $\text{Cs}_{7.0}\text{Na}_{15.7}\text{Ag}_{4.4}\text{Ge}_{131.6}$ , in reasonable agreement with the expected value for Sample II, whereas the Ag content  $x$  was determined from single crystal X-ray refinement to be 5.9(1.0). For sample III the composition was determined from EDS to be  $\text{Cs}_{7.4}\text{Na}_{15.7}\text{Ag}_{4.8}\text{Ge}_{131.2}$ , whereas the Ag content  $x$  was determined from to be 6.7(1.1) from X-ray structural refinements, notably less than the target value of ‘8’. The standard deviations in the compositions determined from EDS measurements are  $\approx 5\%$ . As determined from both X-ray diffraction and EDS measurements, the Ag content in Samples II and III are only marginally different, and both less than  $x = 8$ . As discussed above, a small amount of elemental Ag was present in Sample III, consistent with the value of  $x$  being less than the target value of 8. These results suggest that the value of  $x$  for the solid solubility of Ag in the  $\text{Cs}_8\text{Na}_{16}\text{Ag}_x\text{Ge}_{136-x}$  compounds is  $\approx 7$ . The small difference in the Ag content between Samples II and III is consistent with the fact that the lattice parameter of Sample III is only marginally larger than that of Sample II.

### 4. Conclusions

Framework-substituted type II germanium clathrates have been synthesized for the first time, and the structures of these compounds studied using single crystal X-ray

Table 5  
Selected bond angles for  $\text{Cs}_8\text{Na}_{16}\text{Ag}_x\text{Ge}_{136-x}$  ( $^\circ$ )

Central metal	Angles ( $^\circ$ )		
	Sample I ( $x = 0$ )	Sample II ( $x = 5.9(1.0)$ )	Sample III ( $x = 6.7(1.1)$ )
Ge1	$105.26(2) \times 2$	$105.34(2) \times 2$	$105.40(2) \times 2$
	$108.17(2) \times 1$	$108.06(2) \times 1$	$108.02(2) \times 1$
	$108.87(2) \times 2$	$108.83(1) \times 2$	$108.80(2) \times 2$
	$119.82(0) \times 1$	$119.83(0) \times 1$	$119.83(0) \times 2$
Ge2	$107.10(2) \times 3$	$107.20(2) \times 3$	$107.24(2) \times 3$
	$111.74(2) \times 3$	$111.64(1) \times 3$	$111.60(2) \times 3$
Ge3	$109.47(2) \times 6$	$109.47(0) \times 6$	$109.47(0) \times 6$

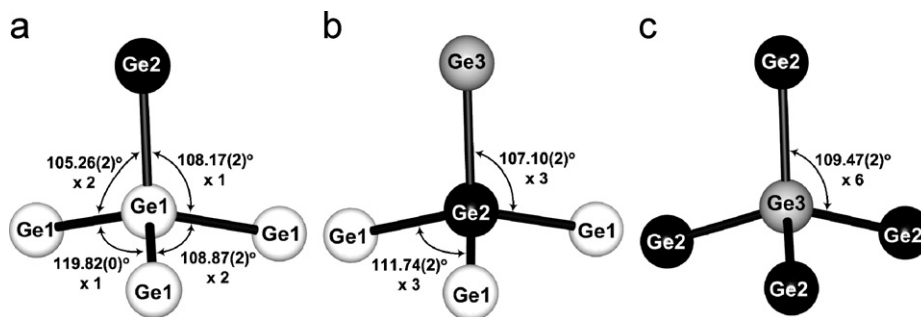


Fig. 4. Local tetrahedral bonding environments of the (a) Ge1 (96g), (b) Ge2 (32e), and (c) Ge3 (8a) sites in  $\text{Cs}_8\text{Na}_{16}\text{Ge}_{136}$ , with bond angles given. The Ge1 site in (a) is the least symmetric, and is the center for the  $\sim 120^\circ$  interior angle of the hexagonal face of the hexakaidecahedra. Ag substitutes preferentially at this site.

diffraction. Single crystal X-ray structural refinements and energy dispersive spectroscopy measurements on  $\text{Cs}_8\text{Na}_{16}\text{AgGe}_{136-x}$  samples both revealed unequivocally that Ag atoms substitute for the framework germanium atoms, and were found to preferentially occupy the most asymmetric 96*g* crystallographic site. No indication from the structural refinements was found for partial occupancy of any of the framework or cation sites in these structures. The large atomic displacement parameters in the type II clathrates can be attributed to large thermal motion of the loosely bound guests inside the framework cages. The lattice thermal conductivities of type II clathrates are in general expected to be low, thus type II clathrates are of interest as potential thermoelectric materials. These results indicate that type II clathrates are indeed stable under framework substitution, and should provide new directions in the synthesis of novel inorganic type II clathrate materials.

### Acknowledgments

G.S.N. and M.B. acknowledge support from the Department of Energy under Grant No. DE-FG02-04ER46145, for synthesis, powder XRD, and data analysis. M.B. also gratefully acknowledges support from the University of South Florida Presidential Doctoral Fellowship.

### Note added in proof

While this manuscript was under review, work was published by Bobev et al. [35] reporting on the synthesis and structural characterization of the type II silicon clathrates  $\text{Rb}_{7.3}\text{Na}_{16}\text{Ga}_{20}\text{Si}_{116}$  and  $\text{Cs}_8\text{Na}_{16}\text{Ga}_{21}\text{Si}_{115}$ , corresponding to simultaneous work on framework substitution in type II clathrates. Their single crystal XRD analysis indicates that Ga substitutes for Si preferentially at the 96*g* site, in agreement with our findings on Ag substitution for Ge, and supporting our suggestion that the 96*g* site is the most susceptible to substitution in type II clathrates.

### References

- [1] J.S. Kasper, P. Hagenmuller, M. Pouchard, C. Cros, *Science* 150 (1965) 1713.
- [2] C. Cros, M. Pouchard, P. Hagenmuller, *J. Solid State Chem.* 2 (1970) 570.
- [3] G.S. Nolas, J.L. Cohn, G.A. Slack, S.B. Schujman, *Appl. Phys. Lett.* 73 (1998) 178.
- [4] G.S. Nolas, in: D.M. Rowe (Ed.), *Thermoelectrics Handbook: Macro to Nano*, CRC Press, Boca Raton, 2006 pp. 33-1.
- [5] A. Saramat, G. Svensson, A.E.C. Palmqvist, C. Stiewe, E. Mueller, D. Platzek, S.G.K. Williams, D.M. Rowe, J.D. Bryan, G.D. Stucky, *J. Appl. Phys.* 99 (2006) 023708.
- [6] J.L. Cohn, G.S. Nolas, V. Fessatidis, T.H. Metcalf, G.A. Slack, *Phys. Rev. Lett.* 82 (1999) 779.
- [7] H. Kawaji, H. Horie, S. Yamanaka, M. Ishikawa, *Phys. Rev. Lett.* 74 (1995) 1427.
- [8] S. Paschen, W. Carrillo-Cabrera, A. Bentien, V.H. Tran, M. Baenitz, Yu. Grin, F. Steglich, *Phys. Rev. B* 64 (2001) 214404.
- [9] G.T. Woods, J. Martin, M. Beekman, R.P. Hermann, F. Grandjean, V. Keppens, O. Leupold, G.J. Long, G.S. Nolas, *Phys. Rev. B* 73 (2006) 174403.
- [10] X. Blase, P. Gillet, A. San Miguel, P. Mélinon, *Phys. Rev. Lett.* 92 (2004) 215505.
- [11] G.S. Nolas, G.A. Slack, S.B. Schujman, in: T.M. Tritt (Ed.), *Semiconductors and Semimetals*, Vol. 69, Academic Press, San Diego, 2001 p. 255.
- [12] P. Rogl, in: D.M. Rowe (Ed.), *Thermoelectrics Handbook: Macro to Nano*, CRC Press, Boca Raton, 2006 pp. 33-1.
- [13] S. Bobev, S.C. Sevov, *J. Solid State Chem.* 153 (2000) 92.
- [14] T. Rachi, K. Tanigaki, R. Kumashiro, J. Winter, H. Kuzmany, *Chem. Phys. Lett.* 409 (2005) 48.
- [15] R. Kröner, K. Peters, H.G. von Schnering, R. Nesper, *Z. Kristallogr. NCS* 213 (1998) 664.
- [16] J. Gryko, R.F. Marzke, G.A. Lamberton Jr., T.M. Tritt, M. Beekman, G.S. Nolas, *Phys. Rev. B* 71 (2005) 115208.
- [17] J. Gryko, P.F. McMillan, R.F. Marzke, G.K. Ramachandran, D. Patton, S.K. Deb, O.F. Sankey, *Phys. Rev. B* 62 (2000) R7707.
- [18] A.M. Guloy, R. Ramlau, Z. Tang, W. Schnelle, M. Baitinger, Y. Grin, *Nature* 442 (2006) 320.
- [19] H.M. Rietveld, *J. Appl. Crystallogr.* 2 (1969) 65.
- [20] R.A. Young (Ed.), *The Rietveld Method*, International Union of Crystallography Monograph on Crystallography, No. 5, Oxford University Press, Oxford, 1993.
- [21] A.C. Larson, R.B. von Dreele, GSAS-General Structure Analysis System, US Government contract (W-7405-ENG-36) by the Los Alamos National Laboratory, which is operated by the University of California for the US Department of Energy, 1992.
- [22] J.A. Kaduk, W. Wong-Ng, G.S. Nolas, *Rigaku J.* 20 (2003) 2.
- [23] CAD4 Operation Manual, Enraf-Nonius, Delft, The Netherlands, 1977.
- [24] G.M. Sheldrick, SHELXL/PC. Version 5. Program for data reduction, structural solution, and refinement of crystal structures. Siemens Analytical X-ray Instruments Inc., Madison, Wisconsin, USA, 1995.
- [25] D.T. Cromer, J.T. Waber, *International Tables for X-ray Crystallography*, Vol. C, Tables 4.2.6.8 and 6.1.1.4, Kluwer Academic Publishers, Dordrecht, 1992.
- [26] G. Cordier, P. Woll, *J. Less-Common Metals* 169 (1991) 291.
- [27] B. Eisenmann, H. Schäfer, R. Zagler, *J. Less-Common Metals* 118 (1986) 43.
- [28] A.P. Wilkinson, C. Lind, R.A. Young, S.D. Shastri, P.L. Lee, G.S. Nolas, *Chem. Mater.* 14 (2002) 1300.
- [29] L. Pauling, B. Kamb, *Proc. Natl. Acad. Sci. USA* 83 (1986) 3569.
- [30] R.D. Shannon, C.T. Prewitt, *Acta Crystallogr. B* 25 (1969) 925.
- [31] G.S. Nolas, D.G. Vanderveer, A.P. Wilkinson, J.L. Cohn, *J. Appl. Phys.* 91 (2002) 8970.
- [32] G.S. Nolas, C.A. Kendziora, J. Gryko, J.J. Dong, C.W. Myles, A. Poddar, O.F. Sankey, *J. Appl. Phys.* 92 (2002) 7225.
- [33] M. Beekman, G.S. Nolas, *Physica B* 383 (2006) 111.
- [34] C.W. Myles, J.J. Dong, O.F. Sankey, *Phys. Stat. Sol. (b)* 239 (2003) 26.
- [35] S. Bobev, J. Meyers Jr., V. Fritsch, Y. Yamasaki, *Proc. Int. Conf. Thermoelectrics* 24 (2006) 48.